Mon. Not. R. Astron. Soc. **000**, 1–12 (000) Printed 31 March 2017 (MN LATEX style file v2.2)

Galactic conformity measured in semi-analytic models

I. Lacerna,[1,2⋆] S. Contreras,[1,3] R. E. González,[1,3] N. Padilla[1,3] and V. Gonzalez-Perez[4]
[1] *Instituto de Astrofísica, Pontificia Universidad Católica de Chile, Av. V. Mackenna 4860, Santiago, Chile*
[2] *Astrophysical Research Consortium, Physics/Astronomy Building, Rm C319, 3910 15th Avenue NE, Seattle, WA 98195, USA*
[3] *Centro de Astro-Ingeniería, Pontificia Universidad Católica de Chile, Av. V. Mackenna 4860, Santiago, Chile*
[4] *Institute of Cosmology and Gravitation, University of Portsmouth, Dennis Sciama Building, Portsmouth PO1 3FX, UK*

arXiv:1703.10175v1 [astro-ph.GA] 29 Mar 2017

ABSTRACT
We study the correlation between the specific star formation rate of central galaxies and neighbour galaxies, also known as 'galactic conformity', out to several Mpc scales using three different semi-analytic models (SAMs). It has been suggested that SAMs may not show the strong signal of conformity measured in observations. In all the models, when the selection of primary galaxies is based on an isolation criterion in real space, we measure a strong galactic conformity where the mean quenched fraction around quenched primary galaxies is higher than that around star-forming primary galaxies of the same stellar mass. The cumulative signal-to-noise ratio, which is used to evaluate the significance and extension in distance of conformity, depends strongly on the SAM. The two-halo conformity is significant as far as $\sim 5\ h^{-1}$ Mpc. The overall signal of galactic conformity decreases when we remove satellites in the selection of primary galaxies. In this case, there is no significant two-halo conformity in two SAMs. For the other SAM, the two-halo conformity is only detected between isolated, central galaxies in relatively low-mass haloes ($M_{\rm halo}< 10^{12.4}\ h^{-1}\ {\rm M}_{\odot}$) and their neighbours. Finally, we explore the case when the secondary galaxies correspond to central galaxies in the SAMs as an attempt to measure the conformity between distinct haloes. Our results show that there is no conformity beyond $\sim 3\ h^{-1}$ Mpc. The conformity measured out to scales of 3–4 h^{-1} Mpc can be related to the environmental influence of large galaxy clusters around near central galaxies.

Key words: galaxies: evolution – galaxies: general – galaxies: haloes – galaxies: star formation – galaxies: statistics

1 INTRODUCTION

The description of physical properties of galaxies with their environment is paramount for understanding galaxy formation. A remarkable case is galactic conformity that is a term used to describe the observed correlation between star formation in central galaxies and in their neighbour galaxies. Weinmann et al. (2006) defined the term of galactic conformity after finding that quenched central galaxies have a higher fraction of quenched satellite galaxies compared to star-forming central galaxies in galaxy groups of similar mass at $z < 0.05$ in the New York University Value Added Catalogue (NYU-VAGC, Blanton et al. 2005), based on SDSS DR2 (Abazajian et al. 2004). Later, Kauffmann et al. (2013) found a galactic conformity effect between low-mass central galaxies with low specific star formation rate (sSFR) or gas content and neighbour galaxies with low sSFR out to scales of 4 Mpc at $z < 0.03$ in SDSS DR7 (Abazajian et al. 2009). These results motivated the distinction of the conformity measured at small separations between the central galaxy and their satellite galaxies within a dark matter halo as one-halo conformity, whereas the signal measured at large separations of several Mpc between the central galaxy and neighbour galaxies in adjacent haloes as two-halo conformity (Campbell et al. 2015; Hearin et al. 2015).

Galactic conformity has been measured both in the local Universe and at higher redshifts. In addition to the results of Weinmann et al. (2006) and Kauffmann et al. (2013), Wang & White (2012) found that red central galaxies have redder satellites than blue centrals of the same stellar mass using SDSS DR7 and SDSS DR8 (Aihara et al. 2011). Phillips et al. (2014) found that satellites are more quenched around massive quenched galaxies compared to a control sample at fixed stellar mass from SDSS DR7. Knobel et al. (2015) confirmed that satellites around quenched centrals are more likely to be environmentally quenched than those around non-quenched centrals using

⋆ E-mail: ialacern@astro.puc.cl

galaxy groups from SDSS DR7 in the redshift range $0.01 < z < 0.06$. Tinker et al. (2017) and Sin et al. (2017) studied the two-halo conformity in SDSS DR7. At higher redshifts, Hartley et al. (2015) found a tendency for passive satellites to be preferentially located around passive central galaxies using the UKIRT Infrared Deep Sky Survey (UKIDSS; Lawrence et al. 2007) Ultra Deep Survey (UDS) with photometric redshifts at $0.4 < z < 1.6$. Kawinwanichakij et al. (2016) found that satellites around quiescent central galaxies are more likely to be quenched compared to the satellites around star-forming centrals from the deep near-infrared surveys ZFOURGE/CANDELS, UDS, and UltraVISTA (McCracken et al. 2012) with photometric redshifts $0.3 < z < 2.5$. They found that the significance of this one-halo conformity signal varies with redshift ($\gtrsim 3\sigma$ for $0.6 < z < 1.6$, whereas it is only weakly significant at $0.3 < z < 0.6$ and $1.6 < z < 2.5$). Berti et al. (2017) reported an excess of star-forming neighbours around star-forming central galaxies, of $\sim 5\%$ on scales of $0 - 1$ Mpc and a two-halo signal of $\sim 1\%$ on scales of $1 - 3$ Mpc using the PRism MUlti-object Survey (PRIMUS; Coil et al. 2011; Cool et al. 2013) with spectroscopic redshifts at $0.2 < z < 1.0$. These signals are weaker than those detected at $z \lesssim 0.05$.

It is still a matter of debate why quenched central galaxies tend to reside preferentially in quenched environments out to several Mpc scales. Kauffmann (2015) suggests that it could be related to AGN feedback that extends beyond the virial radius of massive haloes since they found an excess of massive neighbour galaxies hosting radio-loud AGN around low-mass, quenched central galaxies.

Hearin et al. (2016) studied the correlations between the mass accretion rates of nearby haloes as a potential physical origin for this effect. They found that pairs of host haloes may show correlated assembly histories even when their present-day separation is greater than thirty times the virial radius of either halo. Therefore, these authors suggest that galactic conformity is related to large-scale tidal fields and that its signal should decrease with redshift. If the star formation history of central galaxies is coupled with some host halo property, that could mean that the two-halo conformity is related to the "assembly bias" (Hearin et al. 2015), where the large-scale clustering of dark matter haloes shows a dependence on halo properties beyond the halo mass (e.g. Gao et al. 2005; Wechsler et al. 2006; Zhu et al. 2006; Bett et al. 2007; Gao & White 2007; Wetzel et al. 2007; Li et al. 2008; Angulo et al. 2008; Faltenbacher & White 2010; Lacerna & Padilla 2011, 2012; van Daalen et al. 2012; Hearin 2015; Lin et al. 2016; More et al. 2016; Tojeiro et al. 2016; Zu et al. 2016). In this context, Berti et al. (2017) mention that their observational results are consistent with the predictions of Hearin et al. (2016) and that two-halo galactic conformity is reflecting assembly bias.

However, Paranjape et al. (2015) argued if the conformity measured by Kauffmann et al. (2013) (and probably that by Berti et al. 2017) at projected scales $\lesssim 4$ Mpc in similar stellar mass bins is evidence of assembly bias. Based on results using a mock galaxy catalogue generated from a halo occupation distribution (HOD) function, they say that only at very large separations ($\gtrsim 8$ Mpc) there is a genuine two-halo conformity that is driven by the assembly bias of small host haloes. They suggest that the observed conformity at $\lesssim 4$ Mpc is just because of central galaxies with the same stellar mass can be residing in host haloes of different halo masses. Tinker et al. (2017) reproduced the result of Kauffmann et al. (2013), but they have shown it is mainly driven by contamination in the isolation criterion to select the sample of central galaxies. After removing a small fraction of satellite galaxies, they detect only a small conformity signal out to projected distances of 2 Mpc. They suggest that $\sim 2 - 5\%$ differences in the quenched fractions of neighbour galaxies at projected distances between 1 and 3 Mpc can be produced by mechanisms other than halo assembly bias. Sin et al. (2017) studied in detail the conformity signal measured by Kauffmann et al. (2013). In addition to the misclassification of satellite galaxies as centrals in the isolation criterion, they mention that this signal is strongly amplified by weighting in favour of central galaxies in very high-density regions, and the use of medians to characterize the bimodal distribution of sSFR. They conclude that the large-scale conformity presented in Kauffmann et al. (2013) is a relatively short-range effect that originates from a very small number of central galaxies in the vicinity of just a few very massive clusters, rather than a very long-range effect.

Interestingly, Kauffmann et al. (2013) and also Kauffmann (2015) found a much weaker galactic conformity in synthetic models (semi-analytic models and hydrodynamical simulations) compared to observations. This indicates that there could be physical processes operating in galaxies that are not included in these models. However, Wang & White (2012) mention that the semi-analytic model of Guo et al. (2011) reproduces qualitatively the trends observed between central galaxies and satellites within a projected distance of 300 kpc. Similarly, Sin et al. (2017) have recently found that the semi-analytic models of Henriques et al. (2015) and Guo et al. (2011) show similar results in terms of both the amplitude and the range of the sSFR correlation to their observational results. Furthermore, Bray et al. (2016) claim to have measured a strong signal of galactic conformity using the Illustris simulation (Vogelsberger et al. 2014), which is a large hydrodynamical simulation. They find that the mean red fraction of galaxies around redder neighbour galaxies is higher than around bluer galaxies at fixed stellar mass out to distances of 10 Mpc. These authors conclude that the measured amplitude of the conformity signal depends on the criteria to select central galaxies in observations, projection effects, and stacking techniques.

The aim of this paper is to measure the galactic conformity using three different semi-analytic models (SAMs) since it has been suggested that these type of numerical models may not show the strong signal of galactic conformity in observations. Nevertheless, our goal is not to reproduce the observational signal, but to establish whether these models can account for this effect using different selection criteria. We discuss our results in the perspective of the scale, so that we can obtain a distinction of the conformity measured within small separations from the central galaxy (one-halo conformity) and at large separations, typically larger than 1 h^{-1} Mpc (two-halo conformity).

The outline of the paper is as follows. The descriptions of the three semi-analytic models used in this paper are presented in Section 2. We define the samples and the method to measure the galactic conformity in Section 3. The results

are shown in Section 4. The implications of our results are discussed in Section 5. Finally, our conclusions are given in Section 6.

Throughout this paper we use the reduced Hubble constant h, where $H_0 = 100\,h\,\mathrm{km\,s^{-1}\,Mpc^{-1}}$, with the following dependencies: stellar mass and halo mass in $h^{-1}\,\mathrm{M}_\odot$, physical scale in h^{-1} Mpc, and the specific star formation rate in $h\,\mathrm{yr}^{-1}$, unless the explicit value of h is specified.

2 DATA

In this section we introduce the three galaxy formation models used in this work. All the models were run over the same dark matter simulation, the Millennium-WMAP7 simulation. Similar to the Millennium simulation (Springel et al. 2005), the Millennium-WMAP7 simulation contains 2160^3 particles in a periodic box of 500 h^{-1} Mpc on a side, but with a mass resolution of $9.3 \times 10^8\ h^{-1}\ \mathrm{M}_\odot$ and with a WMAP7 cosmology[1] (Komatsu et al. 2011).

2.1 The semi-analytic models

The objective of this paper is to test if semi-analytic models (SAMs, e.g. Cole et al. 2000) of galaxy formation can reproduce qualitatively the observed galaxy conformity. In this work we use three SAMs; Guo et al. (2013, hereafter G13) that is a version of L-GALAXIES, which is the main SAM code of the Munich group (De Lucia et al. 2004; Croton et al. 2006; De Lucia & Blaizot 2007; Guo et al. 2011; Henriques et al. 2013, 2015), GALFORM in its Gonzalez-Perez et al. (2014, hereafter GP14) incarnation, the main SAM code of the Durham group (Bower et al. 2006; Font et al. 2008; Lagos et al. 2012; Lacey et al. 2016) with a single IMF, and GRP that is a version of GP14, but with a gradual ram pressure stripping instead of an instantaneous stripping of the hot gas in satellite galaxies (see Lagos et al. 2014 for a comparison between GP14 and GRP).[2]

The aim of SAMs is to establish a physically motivated model of how galaxies form and evolve within a cosmological context. Some of these processes are the shock heating and radiative cooling of gas inside dark matter haloes that lead to the formation of galactic discs, feedback from supernovae (SNe), from the accretion of mass onto supermassive black holes and from photoionization heating of the intergalactic medium (IGM), chemical enrichment of the stars and gas, and galaxy mergers driven by dynamical friction within dark matter haloes, which lead to the formation of stellar spheroids and also may trigger bursts of star formation. The models used in this paper have different implementations of each of these processes. By comparing models from different groups we can get insight for which predictions are robust and which depend on the particular implementation of the physics. For a comparison in the performance of the Munich and Durham groups see Contreras et al. (2013) and Guo et al. (2016).

An important difference between these models is the treatment of satellite galaxies. In GP14, a galaxy is assumed to lose its hot gas halo completely once it becomes a satellite; in both GRP and G13, this process is more gradual and depends on the orbit of the satellite. This is going to affect the conformity prediction at small scales (i.e. one-halo conformity), where in GRP and G13 galaxies will be reddened before, but should not affect the results at large scales (i.e. two-halo conformity).

The three models use a Friend-of-Friend group finding algorithm (FOF, Davis et al. 1985) to identify haloes in each snapshot of the simulation that contain at least 20 particles, and then they run SUBFIND on these groups to identify subhaloes within the FOF groups (Springel et al. 2001). The models use different merger tree algorithms, though. G13 build the merger tree of the subhaloes by tracking particles between snapshots to construct the merger tree of their galaxies following Springel (2005), De Lucia & Blaizot (2007) and Boylan-Kolchin et al. (2009). In the case of GP14 and GRP, they use the Dhalo algorithm (Jiang et al. 2014) to build the merger trees. This method attempts to avoid the premature link of haloes which pass through another halo and imposes that the halo mass increases monotonically with the age of the universe (see Jiang et al. 2014 and Guo et al. 2016 for comparisons between halo masses in L-GALAXIES and GALFORM from the Durham group).

3 DEFINITIONS

3.1 Primary galaxies

In this paper, we estimate the fraction of quenched secondary galaxies around primary galaxies. The latter correspond to the most massive or the brightest galaxy in a group (or halo). By following a similar observational approach of Kauffmann et al. (2013, see also Kauffmann 2015), we define a galaxy with stellar mass $M_{\rm stell}$ to be a primary galaxy if there is no other galaxy with stellar mass greater than $M_{\rm stell}/2$ within a given radius. In practice, this is an isolation criterion where we use the 3D positions of galaxies taking into account the periodic boundary conditions in the simulation box. We use three isolation radii in real space: 0.1, 0.5 and 1 h^{-1} Mpc.

3.2 Secondary galaxies

The secondary galaxies correspond to all the galaxies in the vicinity of primary galaxies. The minimum stellar mass for the secondaries is $10^9\ h^{-1}\ \mathrm{M}_\odot$. Recall that due to the isolation criterion, the maximum stellar mass for the secondary galaxies is $M_{\rm stell}/2$ of the primary galaxy ($M_{\rm stell,sec} < M_{\rm stell,prim}/2$) inside the isolation radius.

3.3 Galactic conformity

In order to detect the galactic conformity in the semi-analytic models, we measure the mean fraction of quenched secondary galaxies around quenched (Q) and star-forming

[1] The values of the cosmological parameter of this simulation are: $\Omega_{m0} = 0.272$, $\Omega_{\Lambda 0} = 0.728$, $\Omega_{b0} = 0.0455$, $\sigma_8 = 0.81$, $n_{\rm s} = 0.967$ and $h = 0.704$

[2] The output of GP14 and G13 models are publicly available from the Millennium Archive in Durham `http://virgo.dur.ac.uk/data.php` and in Garching `http://gavo.mpa-garching.mpg.de/Millennium/`.

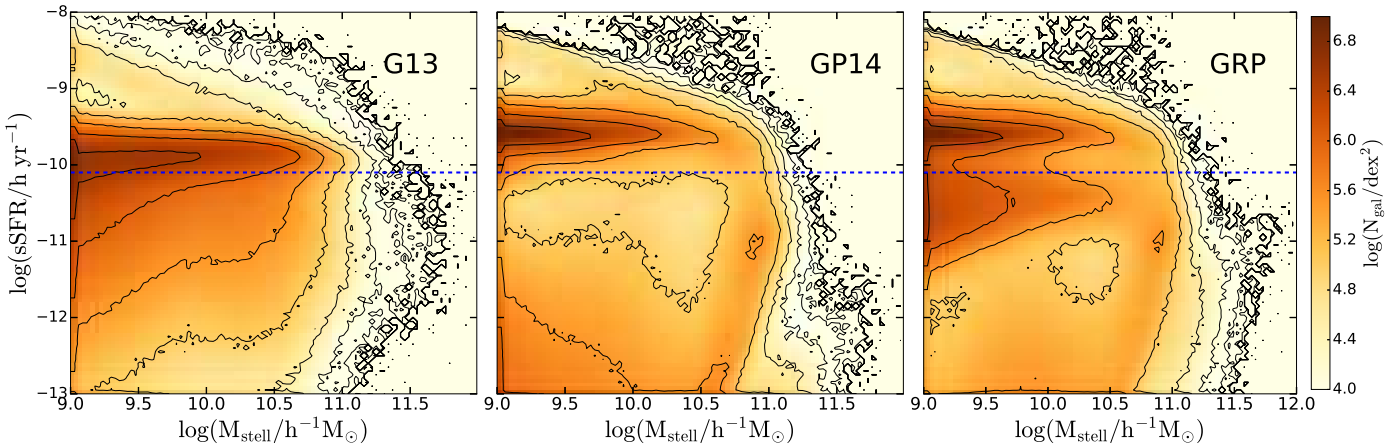

Figure 1. Contours with the distribution of sSFR as a function of stellar mass for the synthetic galaxies of G13 (left-hand panel), GP14 (middle panel), and GRP (right-hand panel). The blue dashed horizontal line is the fiducial value used in this work that roughly separates star-forming and quenched galaxies (above and below the line, respectively). The colour bar indicates the number density of galaxies.

(SF) primary galaxies. We define that there is a galactic conformity signal when the mean quenched fraction of secondaries at a given distance from Q primary galaxies is higher than that around SF primary galaxies of the same stellar mass. Fig. 1 shows the distribution of the specific star formation rate (sSFR, simply defined as the star formation rate normalized by the stellar mass) for the synthetic galaxies of G13, GP14 and GRP as a function of stellar mass. We refer to a galaxy as "quenched" if the sSFR is lower or equal than $10^{-10.1}$ h yr^{-1}. Otherwise, the galaxy is considered as star forming. This value of sSFR is marked as a blue dashed line in Fig. 1. We obtain that the fraction of Q galaxies is similar for the three models using this cut in sSFR (57% for G13, 58% for GP14, and 58% for GRP). We have checked that our results are robust changing this cut by 0.3 and 0.5 dex.

The errors in the estimation of the mean quenched fractions are calculated using the jackknife method (e.g. Zehavi et al. 2002; Norberg et al. 2009). In detail, we split every sample in 120 subsamples and estimate the covariance matrix as follows

$$C(p_i, p_j) = \frac{N-1}{N} \sum_{k=1}^{N} (p_i^k - \overline{p}_i)(p_j^k - \overline{p}_j), \quad (1)$$

where N is the number of subsamples, p_i is the mean quenched fraction around primary galaxies in the ith radial bin, and

$$\overline{p}_i = \frac{1}{N} \sum_{k=1}^{N} p_i^k. \quad (2)$$

Error bars in the figures of Section 4 are estimated using the diagonal of the covariance matrix, i.e., $\sqrt{C(p_i, p_i)}$.

We use the covariance matrix to estimate the cumulative signal-to-noise ratio (S/N) of galactic conformity. The cumulative S/N at a distance r is measured through the difference between the quenched fraction of secondary galaxies around Q and SF primary galaxies as follows

$$(\mathrm{S/N})^2 = B^T A^{-1} B, \quad (3)$$

where $B = p_Q(\leqslant r) - p_{SF}(\leqslant r)$. Here, p_Q and p_{SF} are the mean quenched fraction of secondaries around Q primary galaxies and SF primary galaxies, respectively, considering the radial bins out to r. Furthermore,

$$A^{-1} = (C_Q + C_{SF})^{-1}, \quad (4)$$

where C_Q (C_{SF}) is the full covariance matrix defined in equation (1) for the mean quenched fraction around the Q (SF) primary galaxies. We estimate equation (3) using the elements of A^{-1} out to the radial bin r.

4 RESULTS

4.1 Isolated primary galaxies

Figure 2 shows the mean quenched fraction of secondary galaxies as a function of the distance from primary galaxies in different stellar mass bins. Here the primary galaxies are selected according to the isolation criterion described in Section 3.1 with a radius of 0.1 h^{-1} Mpc (top panels), 0.5 h^{-1} Mpc (middle panels) and 1 h^{-1} Mpc (bottom panels). The mean quenched fraction around Q primaries are shown in solid lines and that around SF primaries are shown in dashed lines. The galactic conformity can be seen as the separation between the solid and dashed lines for a given mass sample (i.e. for the same colour lines).

At small scales ($\lesssim 0.2\ h^{-1}$ Mpc), we detect galactic conformity in the G13 model (left-hand panels), i.e. the mean quenched fraction of secondary galaxies is higher around Q primary galaxies than that around star-forming (SF) primary galaxies of the same mass. The signal is present for the three stellar mass ranges of primary galaxies. On the other hand, the middle panels show the GP14 model with a full quenched population for scales below 0.1 h^{-1} Mpc caused by removing all hot gas in satellites implemented in this model, making impossible to detect galactic conformity at these scales. The GRP model (right-hand panels) shows the stronger galactic conformity at $\lesssim 0.2\ h^{-1}$ Mpc, i.e. larger separations between the solid and dashed lines, especially for the low-mass primaries (red lines).

In general, the mean quenched fraction of secondaries decreases to larger distances out to some scale that is

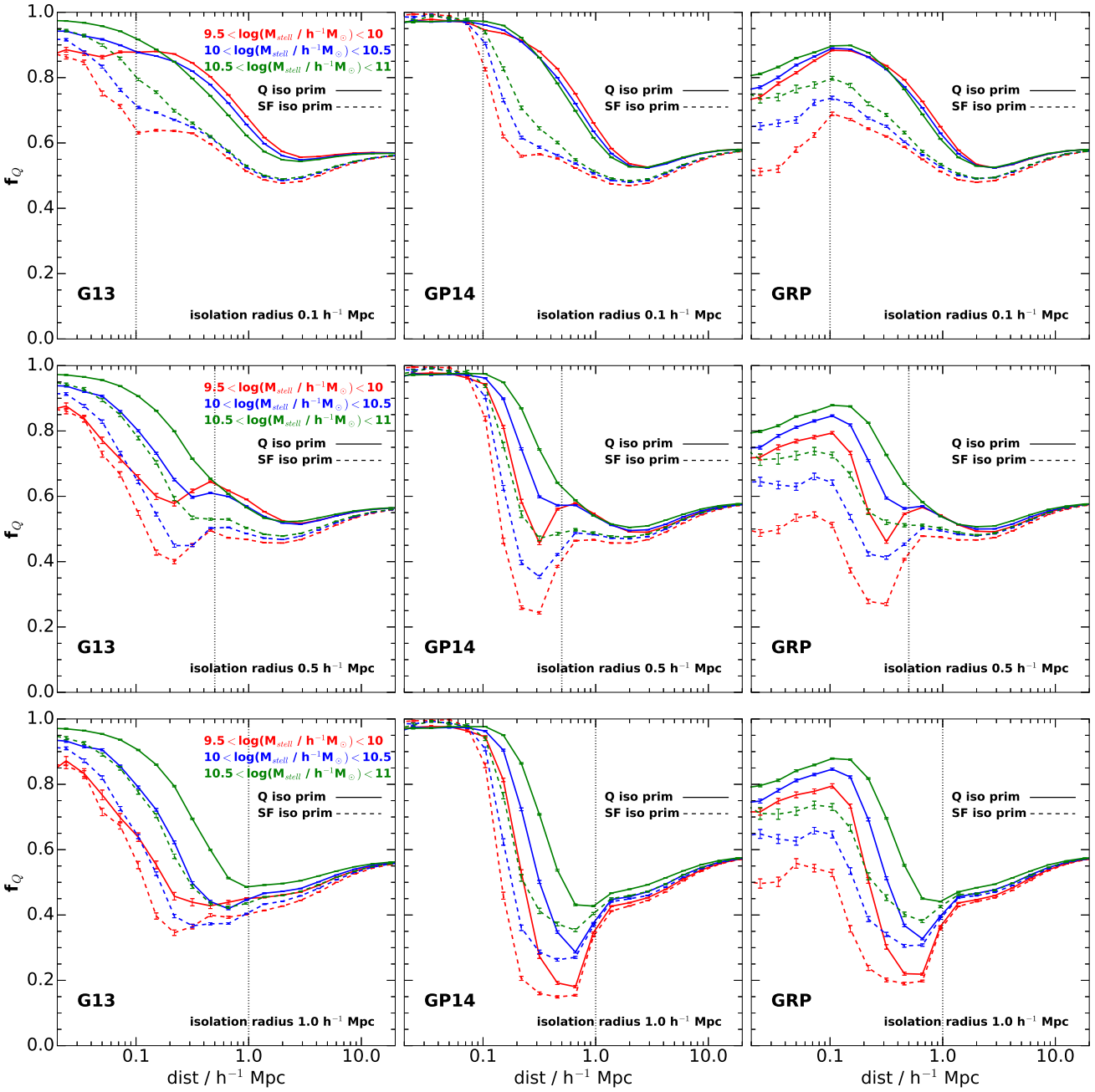

Figure 2. Mean quenched fraction of secondary galaxies as a function of the distance around quenched (Q, solid lines) and star-forming (SF, dashed lines) primary galaxies using the SAMs of G13 (left panels), GP14 (central panels), and GRP (right panels). The colours correspond to different stellar mass bins of primary galaxies indicated in the legend. Primary galaxies are selected according to an isolation criterion in real space (see details in Section 3.1) with a radius of 0.1 h^{-1} Mpc (top panels), 0.5 h^{-1} Mpc (middle panels) and 1 h^{-1} Mpc (bottom panels) shown as a dotted-vertical line in each panel. The galactic conformity can be seen as the separation between the solid and dashed lines for a given mass sample (i.e. for the same colour lines).

strongly dependent on the isolation radius of primary galaxies. At this radius, there is an upturn of the quenched fraction of secondary galaxies. For example, we can see this upturn at ~ 0.1 h^{-1} Mpc, ~ 0.5 h^{-1} Mpc, and ~ 1 h^{-1} Mpc in the top-right, middle-right and bottom-right panels, respectively. Recall that by definition, the secondaries have at most a half of the stellar mass of the primary galaxy inside the isolation radius. Thus, it is more likely to find quenched secondary galaxies at and beyond this scale since the restriction on stellar mass is no longer present from the isolation criteria and, therefore, the mean quenched fraction of secondaries increases. The upturn in the quenched fraction is higher for low-mass primary galaxies (red lines) because the number of secondary galaxies with stellar masses $M_{\rm stell,sec} \geqslant M_{\rm stell,prim}/2$ is higher compared with the case of more massive primaries.

We also detect the two-halo galactic conformity ($\gtrsim 1$ h^{-1} Mpc), but decreases to larger separations from the primary galaxies. This conformity (i.e. the separation between the solid and dashed lines) is lower compared to that in the one-halo conformity and depends on the stellar mass of the primary galaxy. The galactic conformity decreases in the G13 model as we increase the mass of the primary galaxies. At distances of ~ 10 h^{-1} Mpc, there is no galactic conformity regardless the stellar mass and isolation radius, i.e. the mean quenched fractions of secondary galaxies around Q primary galaxies and SF primary galaxies at fixed stellar mass are almost the same. The galactic conformity at large-scales look to be smaller in the GP14 and GRP models compared to the G13 model.

Note that the mean quenched fraction of secondaries slightly increases for scales larger than 3 h^{-1} Mpc in all the SAMs because of quenched satellites in adjacent haloes.

The top panels of Fig. 3 show the cumulative S/N (see Section 3.3) of galactic conformity. This is estimated as the difference in the quenched fraction of all the neighbour galaxies around Q and SF isolated primaries using equation (3). Hereafter, we only use the isolation radius 0.5 h^{-1} Mpc since it is a representative case for selecting primaries (i.e. the overall results at Mpc scales do not change using other radius of isolation). In this figure, an increasing cumulative S/N implies that there is a galaxy conformity signal, while a flat cumulative S/N means no consistent galaxy conformity signal at these scales. In G13 (top-left panel of Fig. 3), the one-halo galactic conformity is stronger for primary galaxies more massive than $M_{\rm stell,prim} > 10^{10}$ h^{-1} $M_\odot$. At larger scales, the galactic conformity becomes stronger between low-mass primary galaxies ($10^{9.5} - 10^{10}$ h^{-1} $M_\odot$) and their neighbours. Table 1 also shows that the cumulative signal-to-noise ratio of this case is higher at 10 h^{-1} Mpc (column S/N(10 h^{-1} Mpc)) compared to the other mass ranges of primary galaxies. The 90% of that signal is reached at 3.6 h^{-1} Mpc whereas this scale is smaller for massive primary galaxies (2.6 h^{-1} Mpc). With the aim to quantify what is the largest extent of the two-halo conformity, we define the maximum distance at which we can still detect a significant galactic conformity signal as S/N(10 h^{-1} Mpc) - 5. This is shown in the last column of Table 1 for the three SAMs. The two-halo conformity for G13 is still significant out to 5.2 h^{-1} Mpc for low-mass primary galaxies and 5.5 h^{-1} Mpc for primaries of intermediate masses. For the most massive primary galaxies, this distance is smaller, 3.7 h^{-1} Mpc.

The two-halo conformity of the GP14 and GRP simulations (top-middle and top-right panels of Fig. 3) are qualitatively similar to that of G13. That is, the highest cumulative S/N is reached in the case between low-mass primary galaxies and their neighbour galaxies. However, the results are quantitatively different. For a given mass range of primaries, the cumulative S/N at 10 h^{-1} Mpc are smaller compared with G13. The 90% of that signal, i.e. where most of the signal is reached, is at a distance much smaller for the GP14 and GRP simulations ($\lesssim 1$ h^{-1} Mpc). The same situation occurs for the distance where the two-halo conformity is still significant. For low-mass primaries, this distance is 5.2 h^{-1} Mpc for G13, but decreases to 3.6 h^{-1} Mpc for GP14 and 1.4 h^{-1} Mpc for GRP. Furthermore, for more massive primaries, this distance is $\lesssim 1$ h^{-1} Mpc for both GP14 and GRP simulations.

Table 1. Conformity signal-to-noise ratio between isolated primary galaxies and secondaries (top panels of Fig. 3). First column shows the mass range for the primary galaxies, the second column is the cumulative S/N at 10 h^{-1} Mpc, the third column is the the distance at which the cumulative S/N is 90% of that at 10 h^{-1} Mpc, and the last column is the maximum distance at which we can still detect a significant galaxy conformity. The latter is defined as S/N($10h^{-1}$ Mpc) - 5. The stellar mass is $\log_{10}$ in units of h^{-1} $M_\odot$, whereas the distance is in units of h^{-1} Mpc.

$\log(M_{\rm stell})$	S/N(10 h^{-1}Mpc)	dist(90%)	dist(max)
G13			
9.5-10	166.7	3.6	5.2
10-10.5	139.0	3.7	5.5
10.5-11	94.0	2.6	3.7
GP14			
9.5-10	115.6	1.2	3.6
10-10.5	103.4	0.4	0.8
10.5-11	75.6	0.4	0.5
GRP			
9.5-10	101.4	0.6	1.4
10-10.5	80.1	0.4	1.1
10.5-11	64.9	0.6	0.7

4.2 Isolated, central primary galaxies

Figure 4 shows the case of isolated, central primaries with an isolation radius of 0.5 h^{-1} Mpc. Therefore, in addition of the isolation criterion used in observations for selecting central galaxies, they are actually central galaxies according to the numerical simulations. The results are similar to those using isolated primaries (middle row panels of Fig. 2) inside the isolation radius. However, it is clear that the galactic conformity is weaker at Mpc scales.

The bottom panels of Fig. 3 show that the cumulative S/N of conformity between the isolated, central galaxies and their neighbours is lower compared to that between isolated primaries and their neighbour galaxies (top panels) for the three SAMs. This means that part of the two-halo conformity detection is polluted by satellites that are classified as primaries using only an isolation criterion for selecting central galaxies (see Kauffmann et al. 2013, Bray et al. 2016, and Tinker et al. 2017 for the same conclusion). We find that the fraction of the low-mass primary galaxies which are actually central galaxies using an isolation radius of 0.5 h^{-1} Mpc is of 96% for G13, 95% for GP14, and 94% for GRP.

For G13, we still find a consistent two-halo conformity signal between isolated, central primaries and secondaries (see also Table 2). The cumulative S/N at 10 h^{-1} Mpc is lower when we include central galaxies in the primary sample, except for the more massive galaxies where this number is almost the same. In this case, we detect a significant two-halo galactic conformity out to ~ 5 h^{-1} Mpc, which is larger than that using only isolated galaxies (3.7 h^{-1} Mpc). However, for GP14 and GRP we do not find a significant two-halo conformity signal between isolated, central primaries and their neighbour galaxies. The 90% of the total signal (at 10 h^{-1} Mpc) is reached at 0.3 h^{-1} Mpc for all the

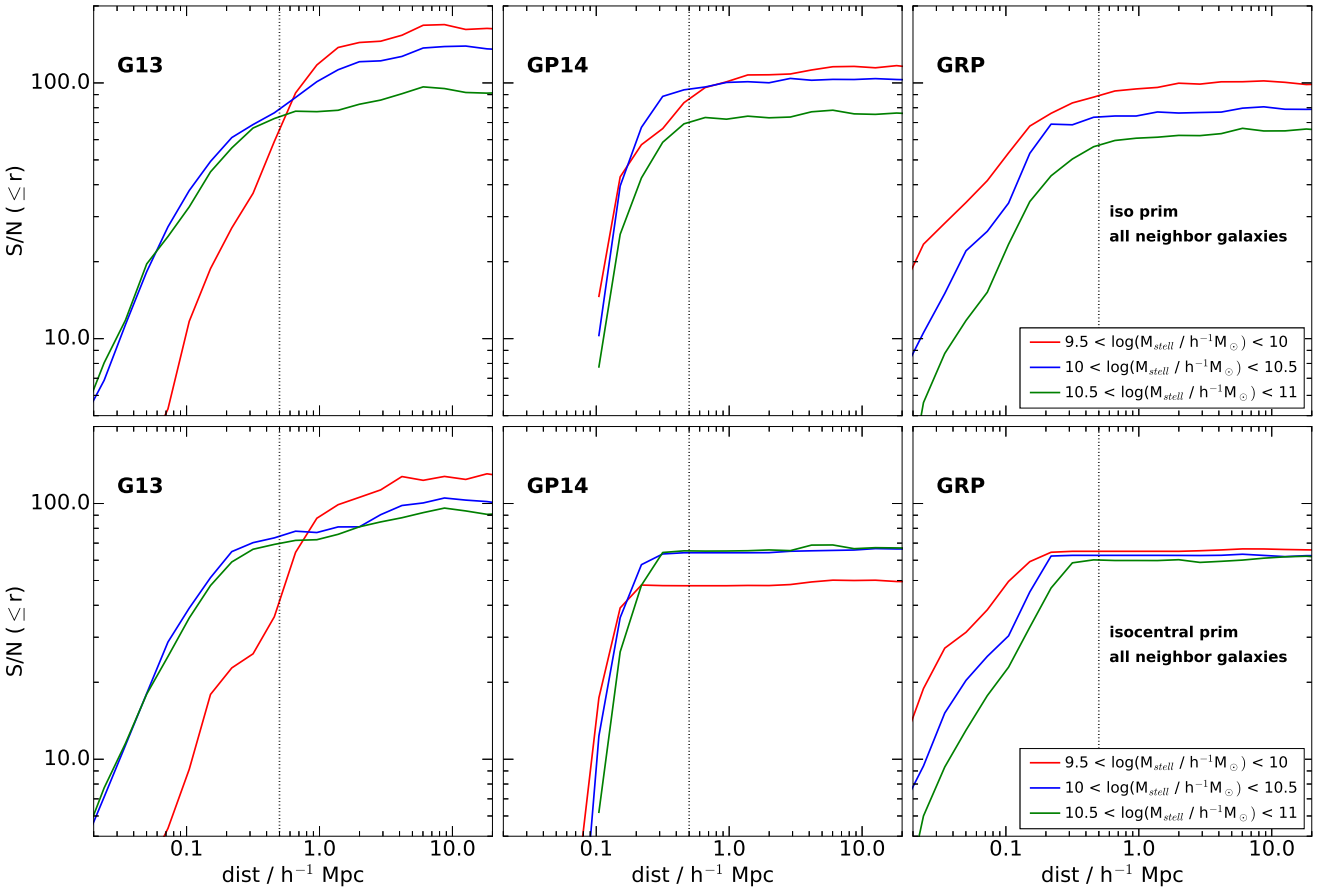

Figure 3. Cumulative signal-to-noise ratio of galactic conformity using the SAMs of G13 (left panels), GP14 (central panels), and GRP (right panels). The difference between the quenched fraction of secondary galaxies around Q and SF primary galaxies with the same stellar mass along with the respective full covariance matrix are used to estimate the cumulative S/N (equation 3). In the top panels, the primary galaxies are selected according to an isolation criterion in real space with a radius of 0.5 h^{-1} Mpc, whereas in the bottom panels they are also central galaxies in the simulations. The isolation radius is shown as a dotted-vertical line in each panel. The colours correspond to different stellar mass bins of primary galaxies indicated in the legend.

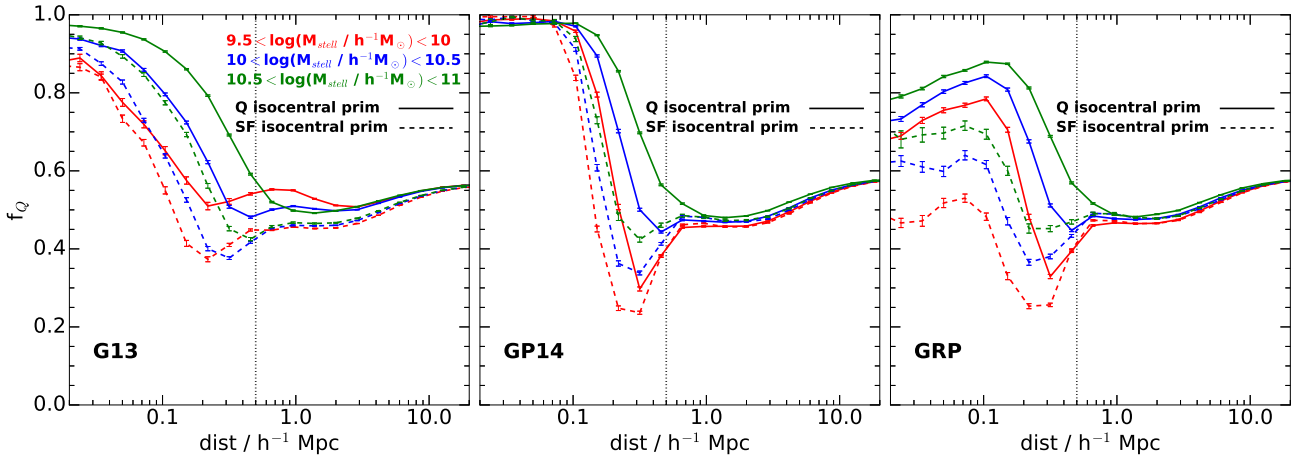

Figure 4. Mean quenched fraction of secondary galaxies as a function of the distance around Q (solid lines) and SF (dashed lines) primary galaxies using the SAMs of G13 (left-hand panels), GP14 (middle panels) and GRP (right-hand panels). Here the primary galaxies are selected according to an isolation criterion in real space with a radius of 0.5 h^{-1} Mpc shown as a dotted-vertical line and, in addition, they are central galaxies in the simulations. The colours correspond to different stellar mass bins of primary galaxies indicated in the legend.

Table 2. Same as Table 1, but for isolated, central galaxies instead of using only isolated galaxies as primaries.

$\log(M_{\rm stell})$	S/N(10 h^{-1}Mpc)	dist(90%)	dist(max)
G13			
9.5-10	126.5	3.0	3.6
10-10.5	104.4	3.5	5.2
10.5-11	95.2	3.2	5.1
GP14			
9.5-10	50.0	0.2	0.2
10-10.5	66.1	0.2	0.3
10.5-11	66.8	0.3	0.3
GRP			
9.5-10	66.3	0.2	0.2
10-10.5	62.4	0.2	0.2
10.5-11	61.4	0.3	0.3

mass ranges of primaries. Likewise, this is the maximum scale where the conformity is still significant. Therefore, using central galaxies as primaries remarkably decreases the two-halo conformity compared to that using only isolated galaxies, but this strongly depends on the physical prescriptions of each model.

The galactic conformity measured at Mpc scales for primary galaxies in G13 could be related with the large scatter in the distribution of halo masses at fixed stellar mass (Paranjape et al. 2015). For this reason, we measure the conformity between massive primary galaxies and their neighbours in three different halo mass ranges for the primaries. We use the case of massive primaries since they show a significant two-halo conformity out to ~ 5 h^{-1} Mpc. For completeness, we also estimate the mean quenched fractions for GP14 and GRP simulations. The halo mass ranges are selected in order to have the same percentage of massive primary galaxies in each halo mass range. The results are shown in Fig. 5. The top panels show the mean quenched fractions around massive Q primaries and massive SF primaries of fixed stellar and halo mass (solid and dashed lines, respectively). The bottom panels show the cumulative S/N for each case. At a given scale, the overall conformity signal decreases notably compared with that in the bottom panels of Fig. 3 (green lines) for each SAM.

The two-halo conformity is not present for the case of massive primaries in massive haloes ($M_{\rm halo}> 10^{12.4}$ h^{-1} M$_\odot$) since the maximum distance at which the cumulative S/N is significant is not larger than 0.1 h^{-1} Mpc for all the SAMs (see Table 3). For massive primary galaxies in haloes of lower mass, this scale is smaller ($\lesssim 3.8$ h^{-1} Mpc) in G13 compared to that without dividing in halo mass (5.1 h^{-1} Mpc). These results support the claim that the two-halo conformity measured for primary galaxies of the same stellar mass is influenced by primaries residing in haloes of different masses. However, we still detect a significant cumulative signal of two-halo conformity of $\sim 25-30$ at 2-4 h^{-1} Mpc between massive isolated, central galaxies in relatively low-mass haloes and their neighbour galaxies in G13.

On the other hand, for a given halo mass, GP14 and GRP show similar mean quenched fractions around massive primaries at scales beyond the virial radius of the primaries (middle top and right top panels of Fig. 5, respectively). Therefore, the two-halo conformity is in general independent of the prescriptions for satellites used in the SAMs. Since the one-halo conformity is relatively strong in the case of GRP, there is no significant conformity beyond 0.2 h^{-1} Mpc using massive primaries at fixed halo mass (see Table 3). For this sample of galaxies in haloes of $M_{\rm halo}< 10^{12.5}$ h^{-1} M$_\odot$ in GP14, the cumulative S/N becomes important just at scales around 0.5 h^{-1} Mpc in contrast to the previous cases when we observed a steep increase in this signal for massive primaries out to ~ 0.3–0.5 h^{-1} Mpc (cumulative S/N > 60). For this reason, the maximum scale of significant conformity between massive primary galaxies in relatively low-mass haloes and their neighbours is around $0.6-0.7$ h^{-1} Mpc, but with a lower cumulative S/N of $\sim 5-10$.

Table 3. Conformity signal between massive isolated, central primary galaxies ($10^{10.5} < M_{\rm stell}/h^{-1}$ M$_\odot < 10^{11}$) and secondaries (Fig. 5). First column is the halo mass range for the primary galaxies, the second column is the cumulative S/N at 10 h^{-1} Mpc, the third column is the the distance at which the cumulative S/N is the 90% of that at 10 h^{-1} Mpc, and the last column corresponds to S/N($10h^{-1}$ Mpc) - 5. The halo mass is $\log_{10}$ in units of h^{-1} M$_\odot$, whereas the distance is in units of h^{-1} Mpc.

$\log(M_{\rm halo})$	S/N(10 h^{-1}Mpc)	dist(90%)	dist(max)
G13			
11-12	33.7	2.8	2.2
12.0-12.4	28.9	4.8	3.8
12.4-14.5	14.6	3.7	0.1
GP14			
11.3-12	10.7	5.5	0.7
12.0-12.5	14.2	3.2	0.6
12.5-14.6	5.8	0.7	0.1
GRP			
11.3-12	9.3	4.6	0.1
12.0-12.5	15.7	1.9	0.2
12.5-14.7	5.0	4.5	–

4.3 Conformity between primaries and central galaxies

In this section we explore the case of galactic conformity between isolated, central galaxies and central galaxies, i.e. we do not include satellite galaxies in the sample of secondary galaxies. Fig. 6 shows the results. The top panels correspond to the mean quenched fraction of central galaxies around isolated, central galaxies for the three SAMs. Of course, this fraction is zero in the one-halo term because we do not include satellite galaxies. Other central galaxies start to appear in the infall region of the primary galaxies (typically between 0.1 and 0.3 h^{-1} Mpc). At larger scales, the conformity is rather weak for GP14 and GRP. However, there are differences in the quenched fraction around Q and SF primaries at fixed stellar mass for G13. For all the SAMs, the quenched fractions decrease monotonically

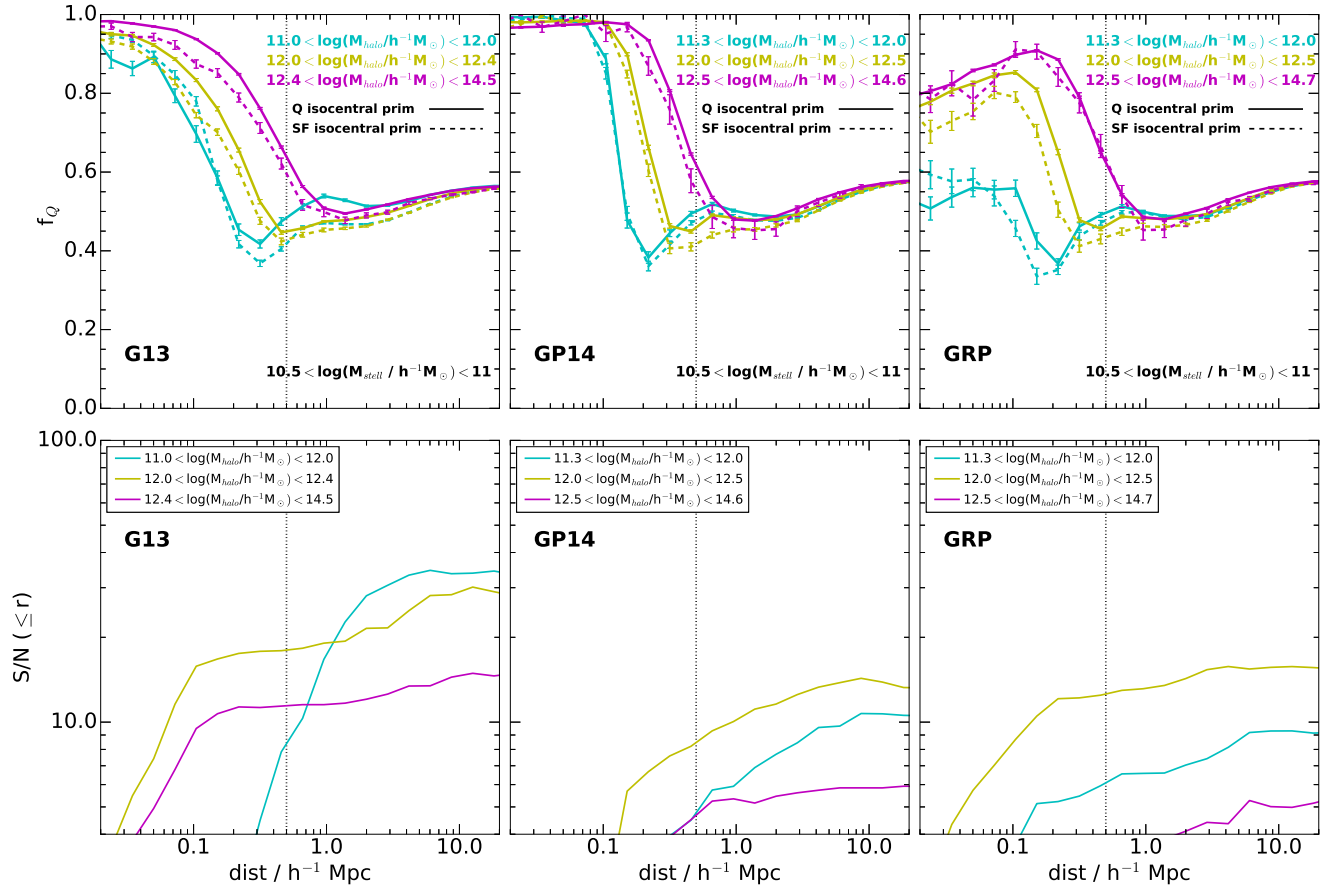

Figure 5. Top panels: mean quenched fraction of secondary galaxies as a function of the distance around Q (solid lines) and SF (dashed lines) primary galaxies using the SAMs of G13 (left-hand panels), GP14 (middle panels) and GRP (right-hand panels). Here the primary galaxies correspond to massive isolated, central galaxies ($10^{10.5} < M_{\rm stell}/h^{-1}$ M$_\odot$ $< 10^{11}$). The colours correspond to different halo mass bins of primary galaxies indicated in the legend for each SAM. These bins were selected in order to have the same percentage of primary galaxies in each halo mass range. Bottom panels: cumulative signal-to-noise ratio of galactic conformity for the cases shown in the top panels. The colours correspond to different halo mass bins of primary galaxies indicated in the legend. The dotted-vertical line in each panel shows the isolation radius.

at Mpc scales since we do not consider satellite galaxies in other haloes (c.f. Fig.4).

As can be seen in the bottom panels of Fig. 6, the cumulative S/N becomes important at $\sim 1\ h^{-1}$ Mpc in G13. This value gets up to ~ 50 and ~ 100 around massive and low-mass primaries at $10\ h^{-1}$ Mpc, respectively. In contrast, the cumulative S/N is always lower than 15 around primaries of all the masses for GP14 and GRP. The overall signal is lower than that using all the neighbour galaxies (centrals and satellites) as secondaries, especially for GP14 and GRP.

5 DISCUSSION

Our finding of one-halo galactic conformity in the semi-analytic models of G13 and GRP between isolated primary galaxies and their neighbour galaxies (Section 4.1) are consistent with the galactic conformity observed in galaxy groups by other authors (e.g. Wang & White 2012; Phillips et al. 2014). That is, the fraction of quenched neighbour galaxies at scales smaller than $\sim$0.3 h^{-1} Mpc is higher for quenched primary galaxies than for star-forming primaries at fixed stellar mass. This shows that SAMs are able to reproduce the observed correlations between central and satellite galaxies. The signal of this correlation depends on the specific model. In the case of GP14, the environmental process of removing, instantaneously, all hot gas in satellites is so strong that nearly all the neighbour galaxies are quenched inside the virial radius of the central galaxy. Therefore, there is no one-halo conformity in this model. Interestingly, a galactic conformity appears for scales larger than 0.1 h^{-1} Mpc in this model.

As a matter of fact, the three models have high cumulative S/N of galactic conformity at scales $> 0.5\ h^{-1}$ Mpc. Therefore, regardless the feedback acting inside the virial radius of central galaxies, a correlation between quenched (star-forming) central galaxies and quenched (star-forming) neighbour galaxies is detected within scales that correspond to the infall region of haloes and beyond. As well as the case of one-halo conformity, the amplitude of this signal is strongly dependent on each SAM. G13 shows the highest two-halo conformity. The three SAMs consistently show low-mass isolated primary galaxies and their neighbours with higher cumulative S/N of conformity at Mpc scales.

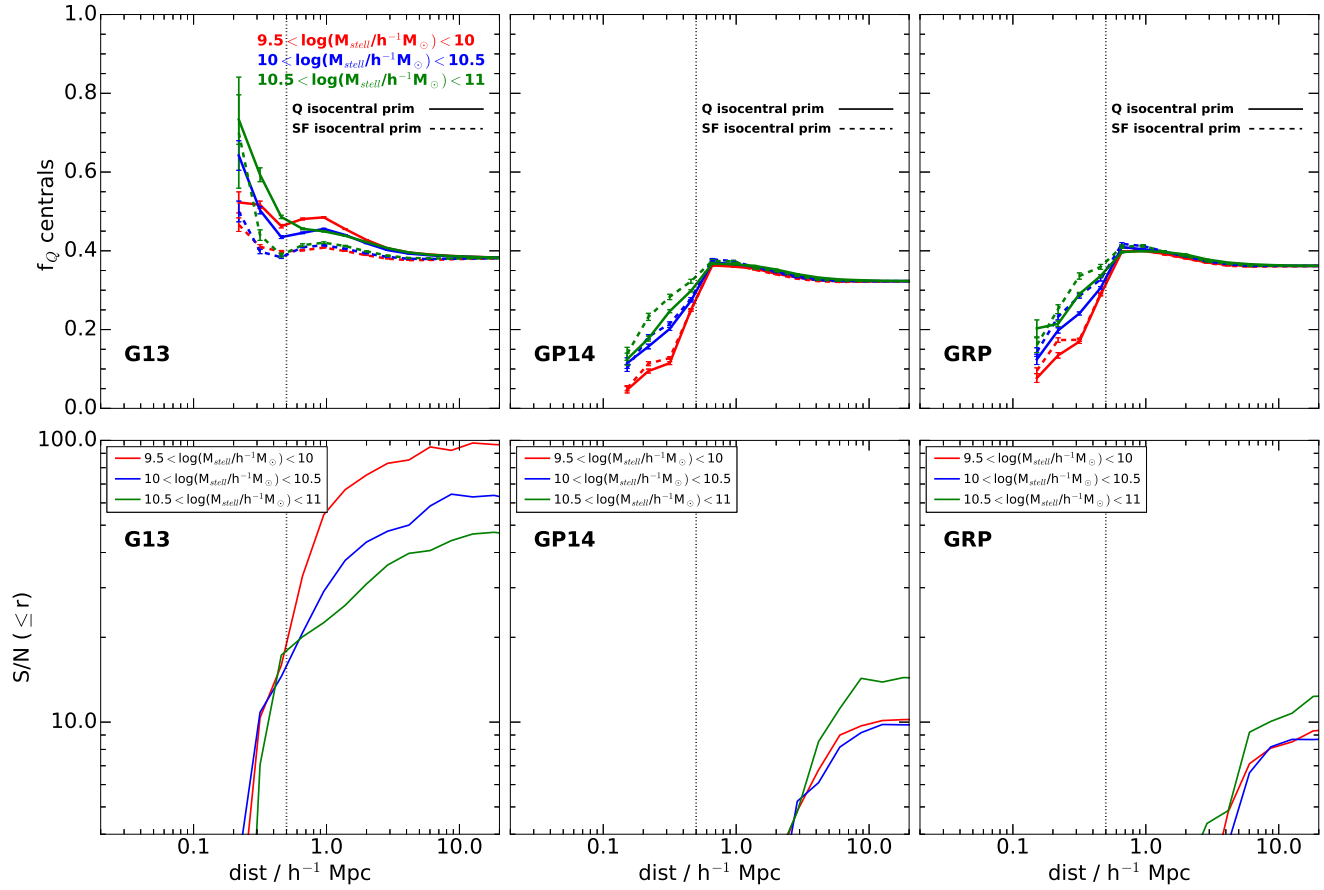

Figure 6. Mean quenched fraction of central galaxies as a function of the distance around Q (solid lines) and SF (dashed lines) primary galaxies using the SAMs of G13 (left-hand panels), GP14 (middle panels) and GRP (right-hand panels). Here the primary galaxies are selected according to an isolation criterion in real space with a radius of 0.5 h^{-1} Mpc shown as a dotted-vertical line and, in addition, they are central galaxies in the SAMs. The colours correspond to different stellar mass bins of primary galaxies indicated in the legend.

Some authors have reported a two-halo conformity in observations (e.g. Kauffmann et al. 2013; Kauffmann 2015; Berti et al. 2017). The chosen criterion of isolated primaries in this work is similar to that used in observations that look for the conformity signal, but we use the 3D information provided by the models to estimate the distance. We expect the signal of conformity to be diluted if the isolation criterion is applied in redshift space. We confirm that the isolation criterion allows some satellite galaxies in the sample of primary galaxies (see Kauffmann et al. 2013; Bray et al. 2016; Sin et al. 2017; Tinker et al. 2017). Although the fraction of satellites in the primary sample is relatively small ($\leqslant 6\%$ for the low-mass primary galaxies), they contribute to increase the cumulative S/N of conformity compared to the case when we use isolated galaxies that are true central galaxies in the SAMs, especially for the low-mass primary galaxies (see Fig. 3). This is consistent with Tinker et al. (2017) and Sin et al. (2017) where the large-scale galactic conformity notoriously decreases after removing a small fraction of satellite galaxies in the primary sample (6.5% and 7%, respectively, for masses between 10^{10} and $10^{10.5}$ $M_{\odot}$) using their group catalogs. Around two-thirds of these satellites are located near large galaxy clusters (Sin et al. 2017).

Two-halo conformity at scales larger than 1 h^{-1} Mpc is not important regardless of the mass of the isolated, central primary galaxies for all the SAMs studied here, except G13. The fact that GP14 and GRP show similar results at large scales although they have different treatment of the hot gas in satellites suggests that other physical recipes of galaxy formation are playing a role in the two-halo conformity. As mentioned in Section 2.1, GP14 and GRP use a different method to build the merger trees compared to G13. In G13, satellite galaxies can be reclassified as central galaxies if they are far enough from the virial radius of the host halo in some snapshots, which is not the case for GP14 and GRP. These models assume that once a galaxy becomes a satellite it will remain as such until it merges with a central galaxy (Guo et al. 2016). We have removed from the primary sample the central galaxies that were ejected in the past in G13. We have found that in this case the overall cumulative S/N decreases, down to a 50 percent for the low-mass primaries. Therefore, central galaxies ejected from their host halo are partially responsible of the high signal of two-halo conformity found in G13.

We also explored the case of conformity between massive isolated, central primary galaxies and their neighbour galaxies at fixed stellar mass and halo mass for the primaries (Fig. 5). The two-halo conformity is detected for mas-

sive primaries in relatively low-mass haloes ($M_{\rm halo} < 10^{12.4}$ h^{-1} $M_\odot$) in G13. The cumulative S/N is weaker (a factor of three) compared to the case of fixing only the stellar mass for the primaries. Our result is qualitatively similar to that of Bray et al. (2016). They find that the mean red fraction of secondaries around redder isolated galaxies is higher than around blue isolated galaxies at fixed halo mass ($M_{\rm halo}$ $< 10^{12}$ h^{-1} $M_\odot$) out to Mpc scales in the Illustris simulation. They use an isolation radius of 0.35 h^{-1} Mpc (0.5 Mpc) in real space. The difference in the mean red fractions is similar to that at fixed stellar mass for the primaries which leads them to conclude that using stellar mass as a proxy for halo mass is unlikely to be biased by this selection technique. However, we note that this would not be valid for central galaxies in massive haloes.

The most striking difference in the cumulative S/N of conformity among the SAMs is when we estimate the mean quenched fraction of central galaxies around isolated, central primaries (Fig. 6). In G13, this value reaches ∼100 for the low-mass primaries, whereas it is lower than 10 for GP14 and GRP. Bray et al. (2016) studied a similar case in Illustris using colour instead of sSFR. They found that the signal of conformity out to $\sim$ 3 Mpc is still present, and nearly identical to the signal in the case with all the neighbour galaxies (i.e. satellites and central) in the secondary sample, but the signal between 3 and 10 Mpc is completely suppressed. This is similar to our result using G13, which in turn is inconsistent with our results for the GP14 and GRP models. In the latter two the cumulative S/N is much lower at all the scales when the satellites are not included in the sample of secondary galaxies. As discussed above, the classification and distinction of central/satellite galaxies in the models can be playing an important role here.

Since in the SAMs the central galaxies are tracing the position of their host haloes, the results shown in Fig. 6 can be thought as an attempt to measure the conformity between haloes. If we assume that stellar mass is a proxy of halo mass and sSFR is a proxy of some physical property of the haloes related to their formation time, this measurement can serve as a link between conformity and the assembly bias. The results using G13 (and also in Bray et al. 2016 and Tinker et al. 2017) show that conformity is not present beyond ~ 3 h^{-1} Mpc for all the masses in this model. Furthermore, in the case of GP14 and GRP, the signal of the proxy of conformity between haloes is very weak at all the scales and masses. It seems difficult that galactic conformity is directly related with a long-range effect, otherwise we should still detect a strong signal of conformity at least between 5 and 10 h^{-1} Mpc. On the other hand, Sin et al. (2017) have found that the conformity out to projected distances of 4 Mpc is primarily related with the environmental influence of large galaxy clusters on central galaxies in high-density environments. Lacerna & Padilla (2011) found that the assembly bias effect can be explained by old, small structures located near massive haloes that are typically at distances out to 4 virial radii ($\lesssim 1.5$ h^{-1} Mpc). These massive haloes could disrupt the normal growth of near small objects and, therefore, affect their virial masses and ages. A more in depth analysis of whether conformity measured in models out to ~ 3 h^{-1} Mpc is reflecting assembly bias will be presented elsewhere.

6 CONCLUSIONS

We have studied the correlation between the sSFR of central galaxies and neighbour galaxies out to several Mpc scales using three SAMs (G13, GP14, and GRP). For that, we measure the mean quenched fraction of secondary galaxies around central (primary) galaxies. The secondary galaxies correspond to all the galaxies in the vicinity of primary galaxies. In all the models we find that the mean quenched fraction at distances larger than 0.5 h^{-1} Mpc around quenched primary galaxies is higher than that around star-forming primary galaxies of the same stellar mass, i.e. we detect galactic conformity, when the selection of primary galaxies is based on an isolation criterion as in observations, but in real space. The signal of conformity, measured as the cumulative S/N, decreases with the mass of the primary galaxies. For a given stellar mass of the primaries, the signal and extension in distance of conformity depends strongly on each SAM. The G13 model shows the higher cumulative S/N and larger extension. For the low-mass primaries ($10^{9.5} < M_{\rm stell}/h^{-1}$ $M_\odot < 10^{10}$), the cumulative S/N is $\sim$ 167 at 10 h^{-1} Mpc and the two-halo conformity is still significant out to ~ 5 h^{-1} Mpc in G13. Although the cumulative S/N is > 100 in the GP14 and GRP models for this stellar mass, the two-halo conformity is significant out to $\sim$ 3.6 and 1.4 h^{-1} Mpc, respectively.

The isolation criterion includes a small fraction of satellites galaxies in the sample of primary galaxies ($\lesssim 6\%$ for low-mass primaries). The overall galactic conformity decreases when we add the condition of central galaxies, according to the information given by the SAMs, in the selection of the primaries. There is no significant two-halo conformity in the GP14 and GRP models in this case. For the G13 model, a half of the cumulative S/N for low-mass primaries is explained by central galaxies that were ejected from other haloes in the past.

We explore if the two-halo conformity in G13 is related with the scatter in the distribution of halo masses at fixed stellar mass. We find that the two-halo conformity is only detected for isolated, central galaxies in relatively low-mass haloes ($M_{\rm halo} < 10^{12.4}$ h^{-1} $M_\odot$). This conformity is still significant out to $\lesssim 4$ h^{-1} Mpc, but the cumulative S/N in the case of fixing both stellar and halo mass is a factor of three weaker compared with the case of fixing only the stellar mass for the primary galaxies.

Finally, we explore the case of conformity when the secondary galaxies correspond to central galaxies in the SAMs as an attempt to measure the correlation of conformity between distinct haloes. Our results show that there is no conformity beyond ~ 3 h^{-1} Mpc for all the mass ranges in the G13 model, and there is a weak two-halo conformity for both GP14 and GRP. It is likely that the conformity measured at scales smaller than 3–4 h^{-1} Mpc is related with the environmental influence of large galaxy clusters on central galaxies hosted by lower mass haloes.

ACKNOWLEDGMENTS

Part of these calculations were performed using the Geryon cluster at the Center for Astro-Engineering UC, part of the BASAL PFB-06, which received joint funding from Anillo

ACT-86, FONDEQUIP AIC-57 and QUIMAL 130008. NP & SC acknowledge support from a STFC/Newton Fund award (ST/M007995/1 - DPI20140114). SC further acknowledges support from CONICYT Doctoral Fellowship Programme.

REFERENCES

Abazajian K. et al., 2004, AJ, 128, 502
Abazajian K. N. et al., 2009, 182, 543
Aihara H. et al., 2011, ApJS, 193, 29
Angulo R. E., Baugh C. M., Lacey C. G., 2008, MNRAS, 387, 921
Berti A. M., Coil A. L., Behroozi P. S., Eisenstein D. J., Bray A. D., Cool R. J., Moustakas J., 2017, ApJ, 834, 87
Bett P., Eke V., Frenk C. S., Jenkins A., Helly J., Navarro J., 2007, MNRAS, 376, 215
Blanton M. R. et al., 2005, AJ, 129, 2562
Bower R. G., Benson A. J., Malbon R., Helly J. C., Frenk C. S., Baugh C. M., Cole S., Lacey C. G., 2006, MNRAS, 370, 645
Boylan-Kolchin M., Springel V., White S. D. M., Jenkins A., Lemson G., 2009, MNRAS, 398, 1150
Bray A. D. et al., 2016, MNRAS, 455, 185
Campbell D., van den Bosch F. C., Hearin A., Padmanabhan N., Berlind A., Mo H. J., Tinker J., Yang X., 2015, MNRAS, 452, 444
Coil A. L. et al., 2011, ApJ, 741, 8
Cole S., Lacey C. G., Baugh C. M., Frenk C. S., 2000, MNRAS, 319, 168
Contreras S., Baugh C. M., Norberg P., Padilla N., 2013, MNRAS, 432, 2717
Cool R. J. et al., 2013, ApJ, 767, 118
Croton D. J. et al., 2006, MNRAS, 365, 11
Davis M., Efstathiou G., Frenk C. S., White S. D. M., 1985, ApJ, 292, 371
De Lucia G., Blaizot J., 2007, MNRAS, 375, 2
De Lucia G., Kauffmann G., White S. D. M., 2004, MNRAS, 349, 1101
Faltenbacher A., White S. D. M., 2010, ApJ, 708, 469
Font A. S. et al., 2008, MNRAS, 289, 1619
Gao L., White S. D. M., 2007, MNRAS, 377, L5
Gao L., Springel V., White S. D. M., 2005, MNRAS, 363, L66
Gonzalez-Perez V., Lacey C. G., Baugh C. M., Lagos C. D. P., Helly J., Campbell D. J. R., Mitchell P. D., 2014, MNRAS, 439, 264
Guo Q. et al., 2011, MNRAS, 413, 101
Guo Q., White S., Angulo R. E., Henriques B., Lemson G., Boylan-Kolchin M., Thomas P., Short C., 2013, MNRAS, 428, 1351
Guo Q. et al., 2016, MNRAS, 461, 3457
Hartley W. G., Conselice C. J., Mortlock A., Foucaud S., Simpson C., 2015, MNRAS, 451, 1613
Hearin A. P., 2015, MNRAS, 451, L45
Hearin A. P., Watson D. F., van den Bosch F. C., 2015, MNRAS, 452, 1958
Hearin A. P., Behroozi P. S., van den Bosch F. C., 2016, MNRAS, 461, 2135
Henriques B. M. B., White S. D. M., Thomas P. A., Angulo R. E., Guo Q., Lemson G., Springel V., 2013, MNRAS, 431, 3373
Henriques B. M. B., White S. D. M., Thomas P. A., Angulo R., Guo Q., Lemson G., Springel V., Overzier R., 2015, MNRAS, 451, 2663
Jiang L., Helly J. C., Cole S., Frenk C. S., 2014, MNRAS, 440, 2115
Kauffmann G., 2015, MNRAS, 454, 1840
Kauffmann G., Li C., Zhang W., Weinmann S., 2013, MNRAS, 430, 1447
Kawinwanichakij L. et al., 2016, ApJ, 817, 9
Knobel C., Lilly S. J., Woo J., Kovač K., 2015, ApJ, 800, 24
Komatsu E. et al., 2011, ApJS, 192, 18
Lacerna I., Padilla N., 2011, MNRAS, 412, 1283
Lacerna I., Padilla N., 2012, MNRAS, 426, L26
Lacey C. G. et al., 2016, MNRAS, 462, 3854
Lagos C. d. P., Bayet E., Baugh C. M., Lacey C. G., Bell T. A., Fanidakis N., Geach J. E., 2012, MNRAS, 426, 2142
Lagos C. d. P., Davis T. A., Lacey C. G., Zwaan M. A., Baugh C. M., Gonzalez-Perez V., Padilla N. D., 2014, MNRAS, 443, 1002
Lawrence A. et al., 2007, MNRAS, 379, 1599
Li Y., Mo H. J., Gao L., 2008, MNRAS, 389, 1419
Lin Y. T., Mandelbaum R., Huang Y. H., Huang H. J., Dalal N., Diemer B., Jian H. Y., Kravtsov A., 2016, ApJ, 819, 119
McCracken H. J. et al., 2012, A&A, 544, A156
More S. et al., 2016, ApJ, 825, 39
Norberg P., Baugh C. M., Gaztañaga E., Croton D. J., 2009, MNRAS, 396, 19
Paranjape A., Kovač K., Hartley W. G., Pahwa I., 2015, MNRAS, 454, 3030
Phillips J. I., Wheeler C., Boylan-Kolchin M., Bullock J. S., Cooper M. C., Tollerud E. J., 2014, MNRAS, 437, 1930
Sin L. P. T., Lilly S. J., Henriques B. M. B., 2017, ArXiv e-prints
Springel V., 2005, MNRAS, 364, 1105
Springel V., White S. D. M., Tormen G., Kauffmann G., 2001, MNRAS, 328, 726
Springel V. et al., 2005, Nature, 435, 629
Tinker J. L., Hahn C., Mao Y. Y., Wetzel A. R., Conroy C., 2017, ArXiv e-prints
Tojeiro R. et al., 2016, ArXiv e-prints
van Daalen M. P., Angulo R. E., White S. D. M., 2012, MNRAS, 424, 2954
Vogelsberger M. et al., 2014, MNRAS, 444, 1518
Wang W., White S. D. M., 2012, MNRAS, 424, 2574
Wechsler R. H., Zentner A. R., Bullock J. S., Kravtsov A. V., Allgood B., 2006, ApJ, 652, 71
Weinmann S. M., van den Bosch F. C., Yang X., Mo H. J., 2006, MNRAS, 366, 2
Wetzel A. R., Cohn J. D., White M., Holz D. E., Warren M. S., 2007, ApJ, 656, 139
Zehavi I. et al., 2002, ApJ, 571, 172
Zhu G., Zheng Z., Lin W. P., Jing Y. P., Kang X., Gao L., 2006, ApJL, 639, L5
Zu Y., Mandelbaum R., Simet M., Rozo E., Rykoff E. S., 2016, ArXiv e-prints